Available at
http://pvamu.edu/aam
Appl. Appl. Math.
ISSN: 1932-9466

AAM Special Issue No. 4 (March 2019), pp. 44 - 53

Applications and Applied Mathematics:
An International Journal
(AAM)

Joule Heat Parameter Effects on Unsteady MHD flow Over a Stretching Sheet with Viscous Dissipation and Heat source

[1]Srinivas Maripala and [2]Kishan Naikoti

[1]Department of Mathematics
Sreenidhi Institute of Science and Technology
Hyderabad, Telangana, India
Email: maripalasrinu@gmail.com;

[2]Department of Mathematics
UCSOU, Osmania University
Hyderabad, Telangana, India
Email:kishan.naikoti@gmail.com;

Received: August 4, 2018; Accepted: October 28, 2018

Abstract

In the present investigation, we studied the effects of heat source and Joule heating parameter on unsteady magneto-hydro-dynamic and heat transfer of a fluid flow over a radiating stretching sheet. The governing partial differential equations of nonlinear with boundary conditions are solved numerically by implicit finite difference method with Gauss Seidel iteration scheme. The obtained numerical solutions of velocity and temperature profiles are discussed and represented graphically. The effects of various parameters on the velocity and temperature profiles are shown graphically and numerical values of physical quantities such as the skin friction coefficient and the local Nusselt number are presented in tabular form.

Keywords: Joule heating parameter; unsteady flow; MHD; Heat transfer; viscous dissipation

MSC 2010 No.: 74F05, 74S20, 76A05, 76W05, 76D05, 80A20

1. Introduction

The fluid flows over a stretching surface have a great application in the process of extrusion, paper production, etc. This is very complicated to comprehend the heat transfer and flow uniqueness of the process. So, the completed product meets the desired quality specifications.

Sakiadis (1961) explains the behavior of viscous fluid due to a moving surface. There are a lot of industrial processes are arose in the flows in porous media. That type of flows contribute to wide spread in industrial applications and in the natural phenomena which exist in the field of geo-thermo-dynamics for the energy recovery, storage thermal energy, grain storage, etc. It is observed that there are so many authors are published several papers on the flow and stretching surfaces of heat transfer problems. In the fluid dynamics one of the major subject is the problem of unsteady and steady laminar flow over a permeable surface because of its importance from both practical point of view and theoretical has been broadly studied. The boundary layer fluid flows over a stretching surface has been investigated by some of the authors Keller and Magyari (2000), Ishak et. al. (2009) and Cortell (2012) under the restrictive cases. Recently, Khader (2014), Srinivas Maripala (2016) studied about the boundary fluid flow and heat transfer over permeable surface with slip conditions and viscous dissipation. In the study of the present paper considered the effects of joule heating parameter and heat source on unsteady MHD flow over a radiating stretching sheet (2015).

2. Analysis of the flow problem

Let us consider the boundary layer flow of unsteady, laminar two-dimensional flow past a continuously porous stretching sheet. The fluid is immersed in an incompressible electrically conducting. It is assumed that external unsteady flow and heat transfer at time t=0. The origin is fixed, the surface is impulsively stretched with velocity $U_\infty(x,t)$ along the x-axis, while y-axis is measured normal to the surface of the plate. The stretching velocity $U_W(x,t)$and the surface temperature $T_\infty(x,t)$ are given by

$$U_\infty(x,t) = ax/(1-ct) \text{ and } T_\infty(x,t) = T_w + bx/(1-ct)\,, \tag{1}$$

respectively, (a, b and c are constants with $time^{-1}$).

Governing equations of this problem can be written as

$$\frac{\partial u}{\partial x} + \frac{\partial v}{\partial y} = 0\,, \tag{2}$$

$$\frac{\partial u}{\partial t} + u\frac{\partial u}{\partial x} + v\frac{\partial u}{\partial y} = v\frac{\partial^2 u}{\partial y^2} - \frac{\sigma \boldsymbol{B_0^2}}{\rho}u\,, \tag{3}$$

$$\frac{\partial T}{\partial t} + u\frac{\partial T}{\partial x} + v\frac{\partial T}{\partial y} = \alpha\frac{\partial^2 T}{\partial y^2} - \frac{1}{\rho C_p}\frac{\partial q_r}{\partial y} - \frac{\mu}{\rho C_p}\left(\frac{\partial u}{\partial y}\right)^2 + \frac{Q}{\rho C_p}(T - T_\infty) + \frac{\sigma H^2 u^2}{\rho C_p}\,. \tag{4}$$

Accompanied by the boundary conditions:

$$U = U_w\,, V = 0, T = T_w \text{ at } y = 0,$$

$$U = U_w = -cx = v_w\,, N = -m\frac{\partial u}{\partial y}\,, T = T_w \quad C = C_w \text{ at } y = 0\,, \tag{5}$$

and $U \longrightarrow 0$, $T \longrightarrow T_\infty$ as y tends to ∞.

In the *x*-axis and y- axis the velocity components u and v are taken. The fluid temperature (T) in the boundary layer, *t* is time, Kinematic fluid viscosity ($v(=\mu/\rho)$), the dynamic viscosity(μ), the fluid density (ρ), the thermal diffusivity(α) , the specific heat at constant pressure (C_p), Heat source parameter (Q) and the radiative heat flux (q_r), To obtain similarity solution for Equations (2)-(5), the variable magnetic field and heat source parameter are assumed to be $B = B_0/\sqrt{1-ct}$ and $Q = Q_0/1-ct$ respectively, (B_0 and Q_0 are constants).

The radiative heat flux (q_r), under Rosseland approximation, has the from

$$q_r = \left(-\frac{4\sigma^*}{3k^*}\right)\partial T^4/\partial y\ . \tag{6}$$

where, Stefan Boltzmann constant (σ^*) and k^* is the absorption coefficient. Expanding T^4 about T_∞ in Taylor's series, we get

$$T^4 = 4\,T_\infty^3\,T - 3\,T_\infty^4\ \text{, (neglecting higher orders)} \tag{7}$$

Substitute Equations (6) and (7) in Equation (4) we get

$$\frac{\partial T}{\partial t} + u\frac{\partial T}{\partial x} + v\frac{\partial T}{\partial y} = \alpha(1+R)\frac{\partial^2 T}{\partial y^2} + \frac{\mu}{\rho C_p}\left(\frac{\partial u}{\partial y}\right)^2 + \frac{Q}{\rho C_p}(T - T_\infty) + Ju^2\ . \tag{8}$$

The governing partial differential Equations (1) – (3) can be reduced to ordinary differential equations by introducing the following similarity transformation

$$\eta = y\sqrt{\frac{U_w}{vx}},\quad \psi = \sqrt{U_w v x}f(\eta),\ \theta(\eta) = (T - T_\infty)/(T_w - T_\infty), \tag{9}$$

The governing equations i.e., equation of continuity is satisfied for stream function $\psi(x,y)$ with the relations

$$u = \frac{\partial\psi}{\partial y} = (ax/(1-ct))f'(\eta)\ ,\ v = -\frac{\partial\psi}{\partial x} = -\sqrt{va/(1-ct)}f(\eta). \tag{10}$$

The equations of the problem defined by (2), (3), (8) and boundary conditions (5) are, then transformed into a set of ordinary differential equations as follows:

$$f''' + ff'' - f'^2 - Mf' - A\left(f' + \frac{1}{2}\eta f''\right) = 0, \tag{11}$$

$$(1+R)\theta'' + \Pr(f\theta' - f'\theta) - \Pr A\left(\theta + \frac{1}{2}\eta\theta'\right) + \Pr(\mathrm{Ec}\,(f''^2) + \gamma\theta) + Ju^2 = 0\ . \tag{12}$$

Then, the boundary conditions are

$$f(0) = 0,\ f'(0) = 1,\ \theta(0) = 1 \ \text{ at } \eta = 0,$$

$$f'(\eta) \text{ tends to } 0,\ \theta(\eta) \text{ tends to } 0 \text{ as } \eta \text{ tends to } \infty\ , \tag{13}$$

where prime denote differentiation with respect to η.

$A(\text{Unsteady parameter}), = c/a$, $M(\text{Magnetic Parameter}) = \frac{\sigma \boldsymbol{B_0^2}}{\rho a}$,

$Ec(\text{Eckert Number}) = U_w^2/c_p(T_w - T_\infty)$, $\gamma(\text{Heat source parameter}) = \mathrm{Q}_0/\rho c_p a$,

$Pr(\text{Prandtal number}) = v/\alpha$, $J(\text{joule heating parameter}) = \frac{\sigma H^2 vGr^{1/2}}{\rho \mathrm{C_p}(T_w - T_\infty)}$,

$Gr(\text{Grashff number}) = \frac{g\beta l^3(T_w - T_\infty)}{v^2}$.

Physical quantities are:

Skin friction coefficient($C_f = 2\tau_w/\rho U_w^2$) ,

Local Nusselt number ($Nu_x = xq_w/k(T_w - T_\infty)$), and

Local Reynolds number($Re_x = U_w x/v$).

3. Numerical Solution

The non-linear ordinary differential equations (11) and (12) subject to the boundary conditions (13) is solved numerically by implicit finite difference method with Gauss Seidel scheme with the Thomas algorithm. The convergence of the method depends on the choice of the initial guesses. The step size 0.01 is used to obtain the numerical solution with five decimal place accuracy as the criterion of convergence. From the process numerical computation, the Skin friction coefficient and Nusselt number which are respectively proportional to $f''(0)$ and $-\theta'(0)$ are presented in tabular form.

Table 1. Values of - $\theta'(0)$ for various values of *A*, *M*, *R*, *Pr* and *J*

A	M	R	J	Pr	MGR(16)	Present
0	0	0	0.01	0.72	0.8086308	0.8086302
				1	1.0000000	1.000000
0	1	0	0.01	0.72	0.6897110	0.6856221
				1	0.8921452	0.8922433
1	0	0	0.01	0.72	1.0832785	1.0832685
				1	3.7645541	3.7654932
1	1	0	0.01	0.7	1.0499175	1.0498256
				1	3.7136611	3.7145612
1	1	1	0.01	0.7	0.7086420	0.7086420
				1	0.8678333	0.8678321

Table 2. Skin friction and Nusselt number for various values of *A, M, R, Pr, γ, J*

A	M	R	Pr	Ec	γ	J	$-\theta''(0)$	$-f''(0)$
0.5	0.5	0.5	0.72	0.1	0.1	0.01	0.654321	1.345962
				0.5			0.558062	1.345623
			1.0	0.1	0.1	0.001	0.807738	1.345644
			3.0				1.532340	1.345956
	1.0		0.72	0.1	0.1	0.001	0.636588	1.498564
	3.0						0.61452	1.569852
		1.0					0.556213	1.345666
		2.0					0.485652	1.345898
1.0							0.800365	1.497214
2.0							0.911452	1.619581
						0.001	0.455212	1.349621
						1.000	0.345982	1.375123

4. Results

The governing Equations (11) and (12) subjects to the boundary conditions represented in the Equation (13) are solved numarically. The numerical values of the velocity, temperature, local skin friction coefficients and rate of heat transfer are obtained for different values of Unsteady parameter *A*, magnetic parameter *M*, Radiation parameter *R*, Joule heating parameter *J* and heat in generation parameter γ for a Prandtl number 0.73. Detailed numerical results for the velocity, temperature are explained graphically in Figures 1-11 respectively. Local skin friction coefficients and rate of heat transfer associated with the different values of related parameters are shown in tabular form.

From table 1 the heat transfer coefficient increases with an increase of Prandtl number. Effects of MHD parameter *M*, unsteady parameter *A* and joule parameter *J* on Skin friction coefficient $f''(0)$ and Nusselt number $\theta''(0$ are shown in table 2. It is noticed that as the radiation parameter R increases the magnitude of the Nusselt number $-\theta''(0)$ decreases. It is observed that as the Prandtl number *Pr* increases the magnitude of the Nusselt number $-\theta''(0)$ increases. But Skin Friction Coefficient remains constant with increasing values of Radiation Parameter and Prandtl Number. Joule parameter *J*, increase the Skin friction coefficient values and decrease the Nusselt number values.

From Figures 1, 2 and 3 observed that the effects of MHD parameter *M*, unsteady parameter *A* and Joule parameter *J* on the velocity profiles. As expected, the velocity profiles increase with the increase in *M*. When *M* increases, it will also increase the velocity profiles. Thus, the rate of heat transfer at the surface decreases with the presence of magnetic parameter and unsteadiness parameter. From figure 3, Joule heating parameter *J* increase the velocity profiles as it increases.

Figures 4 and 5 depict temperature profiles for various values of Prandtl number *Pr* and Unsteadiness parameter *A*. It is noticed that an increase in *Pr* results a decrease of the thermal boundary layer thickness. Figures 4 and 5 show that the thermal boundary layer thickness

decreases as *Pr* or *A* increases with increasing temperature gradient at the surface. Thus, the heat transfer rate at the surface increases with increasing values of *Pr* or *A*.

The temperature profile for various values of magnetic parameter *M*, radiation parameter *R*, Eckert number *Ec*, and heat source parameter *Q* are presented in Figures 6–8 respectively. Figure 6 and 7 show effects of magnetic parameter *M* and radiation parameter *R* on the temperature profiles respectively. From these figures it can be seen that the absolute value of the temperature gradient at the surface decreases with an increase in *M* or *R*. So, the heat transfer rate at the surface decreases as *M* or *R* increases. As *R* increases the temperature profile also increases.

Figure 8 shows the effect of viscous dissipation parameter *Ec* on temperature profile. As *Ec* increases, the temperature profile also increases; The Temperature profiles for various values of heat source parameter γ are presented in Figure 9. As γ increases, the temperature profiles also increase. It can be seen that the absolute value of temperature gradient at the surface decreases with an increase in *M*, *R*, *Ec* and heat source parameter γ.

Figure 10 represents the effect of Joule heating parameter *J* on temperature field while controlling parameters are MHD parameter *M*, Radiation parameter *R* and heat source parameter *Q*. As Joule heat parameter produce temperature in the conductor therefore temperature of the fluid increase associated with the increasing values of Joule parameter *J*.

5. Conclusion

The governing equations and subject to the boundary conditions represented in the equation and are solved numerically. The numerical values of the velocity, temperature, local skin friction coefficients and rate of heat transfer are obtained for different values of parameters. Specially, Joule heating parameter on temperature field while controlling parameters are MHD parameter, Radiation parameter and heat source parameter. As Joule heat parameter produce temperature in the conductor therefore temperature of the fluid increase associated with the increasing values of Joule parameter.

REFERENCES

Abbas, Z., Hayat, T. (2008). Radiation effects on MHD Flow in a porous space. *International journal of Heat and Mass Transfer*, Vol.51, pp.1024–33.

Chen, CH. (2010). On the analytic solution of MHD flow and heat transfer for two types of visco elastic fluid over a stretching sheet with energy dissipation *International Journal of Heat and Mass Transfer*, Vol.53, Issues 19-20, pp.4264–73.

Chiam, T.C. (1995). Hydro magnetic flow over a surface stretching with a power law velocity. *International Journal of Engineering Science*, Vol.33(3), pp.429–435.

Cortell, R. (2012). Combined effect of viscous dissipation and thermal radiation on fluid flows over a non-linearly stretched permeable wall. *Meccanica*, Vol. 47(3), pp.769-781.

Fang, T., Zhang, J., and Zhong, Y. (2012). Boundary layer flow over a stretching sheet with variable thickness. *Appl Math Comput* ; Vol.218(13). pp.7241–52.

Ghaly, A.Y. (2002). Radiation effects on a certain MHD free convection flow. *Chaos Solitons Fractals*, Vol.13, pp.1843–50.

Ishak,.A., Nazar, R., Pop, I. (2009). Heat transfer over an unsteady stretching permeable surface in with prescribed wall temperature. *Nonlinear Anal. RWA*. Vol.10, pp. 2909-2913.

Khader.MM (2014). Laguerre collocation method for the flow and heat transfer due to a permeable stretching surface embedded in a porous medium with a second order slip and viscous dissipation. *Appl. Math. Compute*. Vol.243, pp.503-513.

Liao, S. (2010). A new branch of solutions of boundary layer flows over an impermeable stretched plate. *Int J Heat Mass Trans*, Vol.48, pp.2529–39.

Machireddy, Gnaneswar, a Reddy, Polarapu Padma, and, Bandari Shankar (2015). Effects of viscous dissipation and heat source on unsteady MHD flow over a stretching sheet. *Ain Shams Engineering Journal*, Vol.6, pp.1195-1201.

Magyari, E., Keller, B. (2000). Exact solutions for self similar boundary layer flows induced by permeable stretching walls. *Eur. J. Mech. B-Fluids* Vol.19, pp.109–22.

Raptis, A. (2004). Effect of thermal radiation on MHD flow. *Appl Math Comput*.Vol.153, pp.645–649.

Sakiadis, B.C. (1961). Boundary layer behaviour on continuous solid surface I, boundary-layer equations for two dimensional and axisymmetric flow. *AIChE J*. Vol.7., Issue.1, pp.26– 28.

Salleh, M.Z., Nazar, R., Pop, I. (2010). Boundary layer flow and heat transfer over a stretching sheet with Newtonian heating. *J Taiwan Inst Chem Eng.* Vol.41: pp.651–655.

Subhashini S.V., Samue,l N., Pop, I. (2011). Effects of Buoyancy assisting and opposing flows on mixed convection boundary layer flow over a permeable vertical surface. *Int Commun Heat Mass Trans*, Vol.38:pp.499–503.

Srinivas, Maripala, Kishan, .N. (2016). MHD effects on micropolar nanofluid flow over a radiative stretching surface with thermal conductivity. *Advances in Applied Science Research. Vol.7*(*3*), pp.73-82.

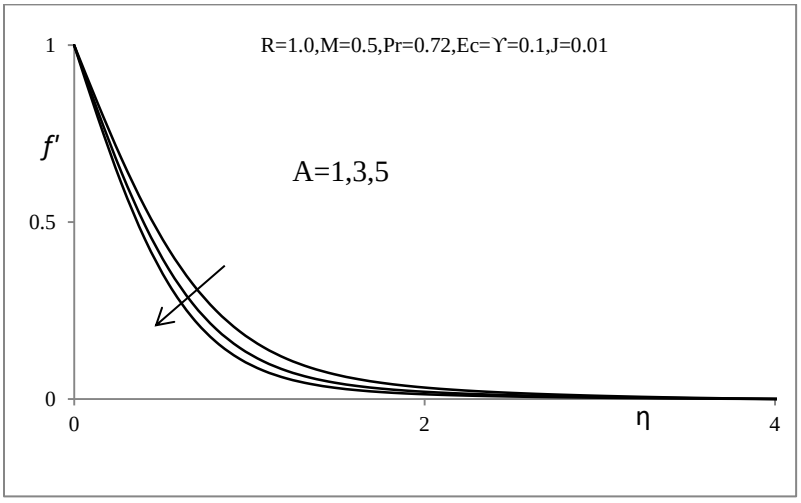

Figure 1. Velocity profiles for different values of *A*

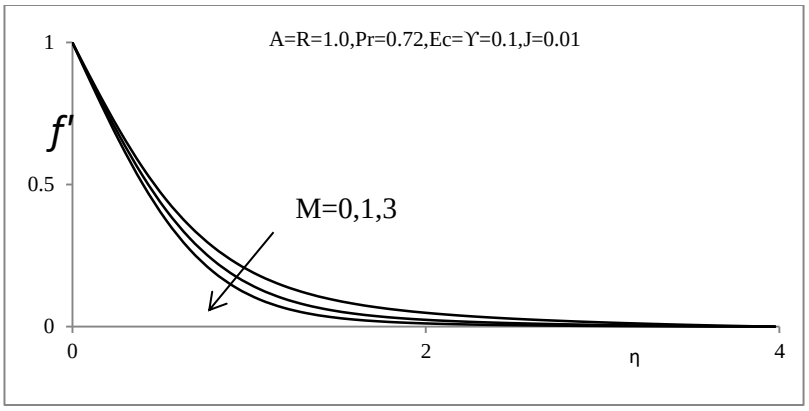

Figure 2. Velocity profiles for different values of *M*

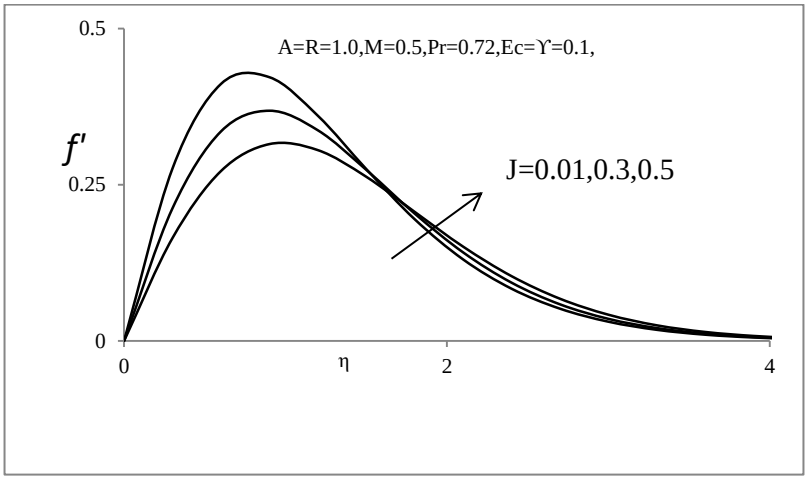

Figure 3. Velocity profiles for different values of *J*

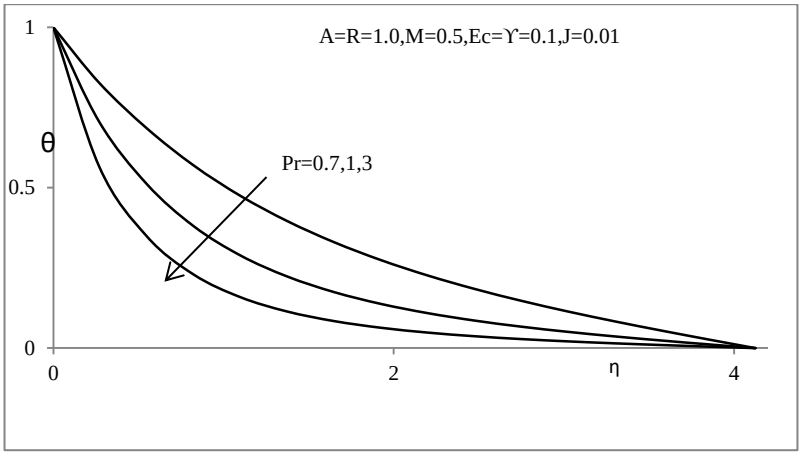

Figure 4. Temperature distribution for various values of *Pr*

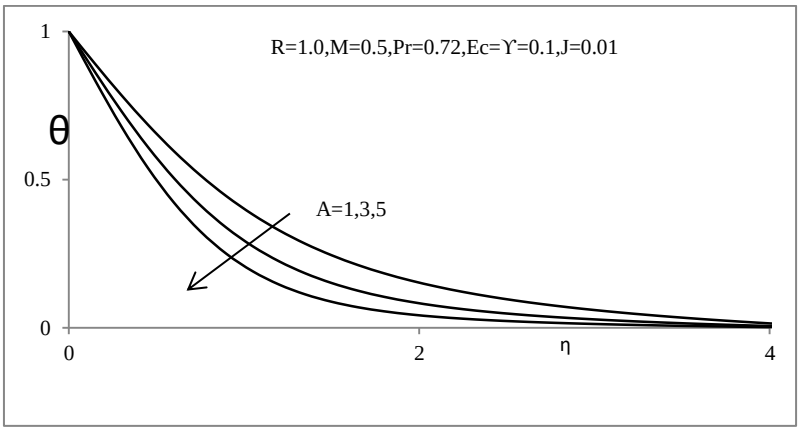

Figure 5. Temperature distribution for various values of *A*

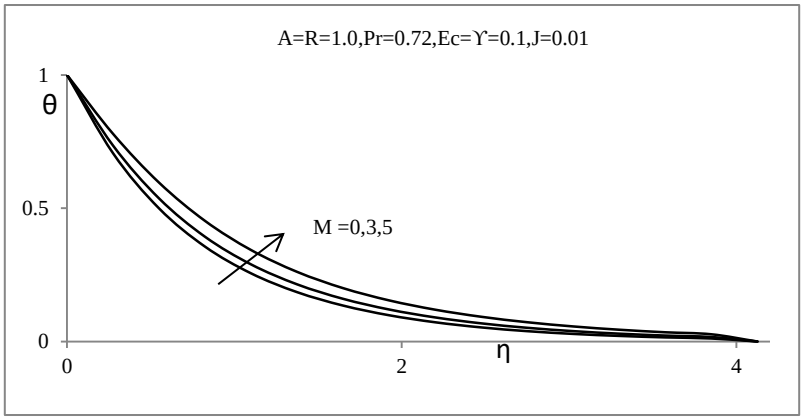

Figure 6. Temperature distribution for various values of *M*

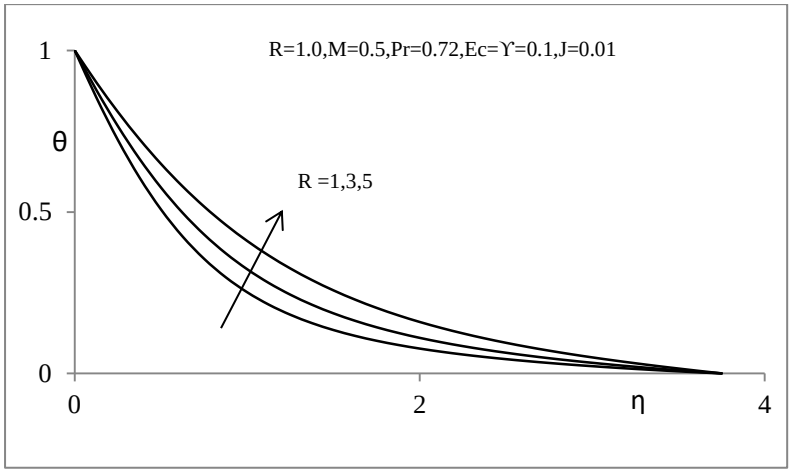

Figure 7. Temperature distribution for various values of *R*

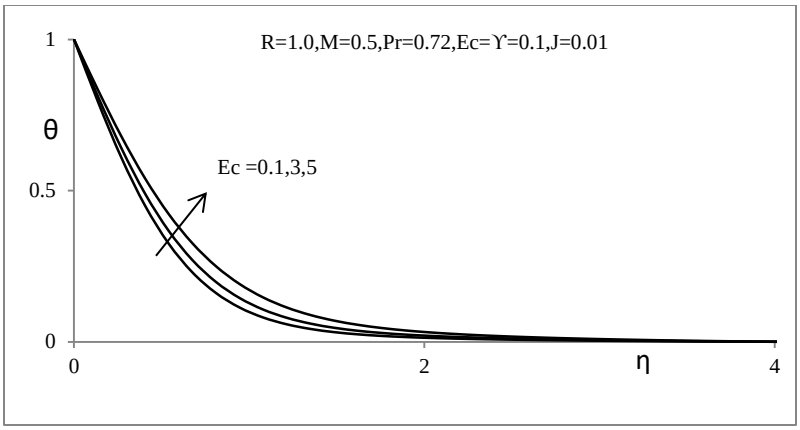

Figure 8. Temperature distribution for various values of *Ec*

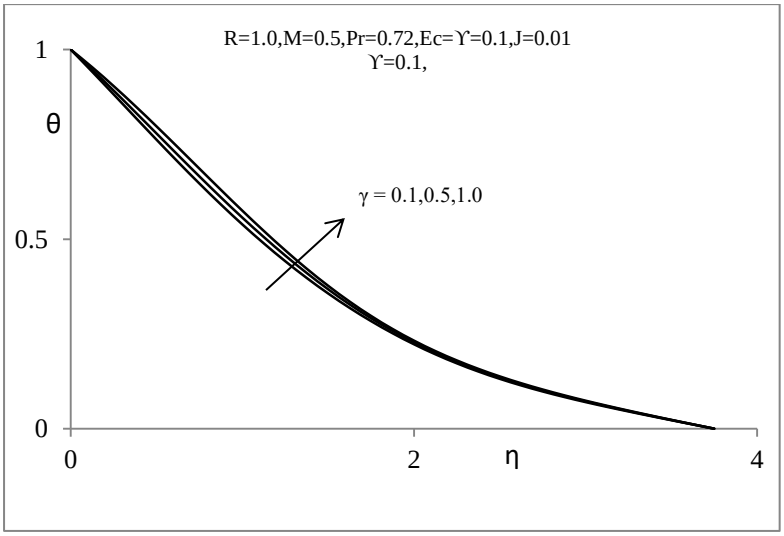

Figure 9. Temperature distribution for various values of γ

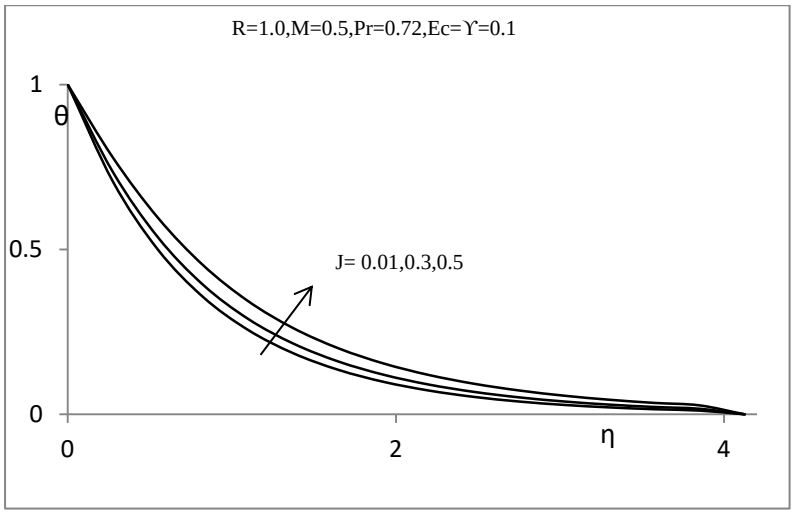

Figure 10. Temperature distribution for various values of *J*